Modification of Carbon Nanotubes Using Poly(vinylidene fluoride) with Assistance of Supercritical Carbon Dioxide: The Impact of Solvent

Linghao He,[†,‡] Xiaoli Zheng,[†] and Qun Xu*[,†]

College of Materials Science and Engineering, Zhengzhou University, Zhengzhou 450052, China, and Henan Provincial Key Laboratory of Surface & Interface Science, Zhengzhou University of Light Industry, Zhengzhou 450052, China

Received: December 07, 2009; Revised Manuscript Received: January 27, 2010

We report herein a typical piezoelectric polymer, poly(vinylidene fluoride) (PVDF) to be successfully wrapped on single-walled carbon nanotubes (SWCNTs) using a simple supercritical carbon dioxide (SC CO_2) antisolvent-induced polymer epitaxy method. Our study focused on the effect of different solvents on the morphology of PVDF wrapping on SWCNTs. Three organic solvents, dimethyl sulfoxide (DMSO), *N*,*N*-dimethylformamide (DMF), and *N*,*N*-dimethylacetamide (DMAc) were chosen for PVDF. When DMSO was used as solvent, the decorating degree of PVDF on the surface of SWCNTs increases significantly with the increase of SC CO_2 pressure, and nanocrystals wrapping on SWCNTs can be observed at high pressure. FTIR and Raman spectra indicated that there exist interactions between SWCNTs and PVDF chains. What's more, FTIR results also show that there exists a transformation from the β-phase to the α-phase of PVDF in DMSO with the assistance of SC CO_2, which is similar to the action of elongation/shear flow field. It indicated that the α-phase is the predominant form occurring on the surface of SWCNTs after treatment with SC CO_2. And the helical structure on SWCNTs observed from the TEM image reflected the alternate trans- and gauche-bond conformation of the α-form. When DMF or DMAc was used as the solvent, although nanocrystal wrapping and helical structure was not visible, the samples had more excellent dispersion than that in DMSO. Particularly, for DMF, a typical network structure was observed, which is similar to a spider web. Therefore, this work supplies a clue that the various morphologies of nanohybrid structure can be obtained just by changing the solvent during the treatment process of SC CO_2, and accordingly, the tailored nanohybrid structure are promising and important for functional design as a basic component in microfabrication and other fields.

Introduction

Due to their nanometer size, high aspect ratios, and more importantly, extraordinary mechanical strength and high electrical and thermal conductivity, carbon nanotubes (CNTs) have been considered ideal candidates to substitute for the conventional nanofillers in multifunctional polymer nanocomposites.[1−6] However, it is very difficult to achieve homogeneous dispersion of CNTs within a polymeric matrix because the as-prepared CNTs usually aggregate into bundles and/or entangle together. To overcome these limitations and broaden their applications in practice, functionalization of CNTs is necessary. The chemical functionalization techniques and noncovalent wrapping methods have been widely studied. The former technique involves the covalent attachment of chemical groups through reactions onto the π-conjugated skeleton of CNTs, by which the structure integrity of CNTs is often disrupted and therewith the electrical and mechanical properties of CNTs decrease sharply.[7−11] For the latter noncovalent wrapping methods, the electronic network of the tubes can be maintained, whereas the noncovalent interaction between CNTs and wrapping molecules is not strong enough.[12−19]

As functionalization of CNTs is growing popular in nanotechnology, many new green techniques have been employed. Supercritical fluids (SCFs) have been widely used in materials science due to their special properties such as low viscosity, high diffusivity, and near zero surface tension.[20] Among SCFs, supercritical CO_2 (SC CO_2) is the most popular one because it is nonflammable, nontoxic, inexpensive, and naturally abundant and has consequently been promoted as a sustainable solvent.[21,22] On the other hand, the solubility of SC CO_2 is poor for many polymers but very high in many solvents, which will lead to a decrease of the solvent strength of organic solvent; i.e., SC CO_2 can act as an antisolvent to enhance the precipitation or absorption of polymers on the surface of CNTs.[23−27] In our previous study, we have successfully achieved the modification of CNTs with polyethylene (PE), poly(ethylene glycol) (PEG), and poly(vinyl alcohol) (PVA) using a simple SC CO_2 antisolvent-induced polymer epitaxy method (SAIPE method).[25−27] These results motivated us to go on investigating other typical polymers and study their modification on CNTs with assistance of SC CO_2.

Fluorinated polymers have extensive application prospects in material science. A well-known polymer in this family is poly(vinylidene fluoride) (PVDF).[28] This polymer has received much attention due to its excellent chemical resistance, mechanical strength, and piezoelectric properties and then has been widely used in diverse fields as transducers for sensitive scientific instruments and pipes for caustic chemical byproducts.[29−33] PVDF is a semicrystalline thermoplastic polymer with five distinct crystal polymorphs depending on the crystallization conditions, including the nonpolar α-phase, polar β- and γ-phases, and δ- and ε-phases.[31] The different crystal phases are associated with the varying

* Corresponding author. E-mail: qunxu@zzu.edu.cn. Tel.: +86 371 67767827. Fax: +86 371 67767827 .
† Zhengzhou University.
‡ Zhengzhou University of Light Industry.

10.1021/jp911621y
Published on Web 04/07/2010

properties of polymer. The first two are the main crystalline phases. The α-phase has an alternating trans- and gauche-bond conformation, as well as excellent mechanical properties. These properties make α-phase PVDF a good electro-optical storage material, which can be used for specific optical, chemical, electronic, and solar energy devices.[32] The β-phase has an all-trans conformation comprising fluorine atoms and hydrogen atoms on the opposite sides of the polymer backbone. This specific conformation could result in a net nonzero dipole moment and so the β-phase is the strongest polar phase among all other crystals. And it can be used extensively in piezoelectric, pyroelectric, and ferroelectric fields.[33] In recent years, study on how to control and improve the content of α-phase or β-phase has been developed widely. It has been reported that there exists a phase transformation between the α-form and β-form by stretching the PVDF film.[34] And some reported studies showed that polymer morphology could be affected by supercritical carbon dioxide (SC CO_2) as well.[35,36] Therefore, we would like to not only study the effect of different solvents on the morphology of PVDF on CNTs with assistance of SC CO_2 but also further investigate the effect of SC CO_2 on the transformation of PVDF crystal phase in this study.

Experimental Section

Materials. The single-walled carbon nanotubes (SWCNTs) were supplied by Carbon Nano Materials R&D Center, Chengdu Desran Technology Co., Ltd. (China), with a purity of 80 wt %. They were purified as follows: proper quantities of crude SWCNTs were added into a three-necked flask containing sulfuric acid and nitric acid in the ratio of 3:1 by volume. The suspension was sonicated in an ultrasonic bath for 40 min and then heated to 120 °C and refluxed for 3 h. After centrifugation and later washing with hot distilled water until pH 7.0, the purified SWCNTs were dried in a vacuum oven at 35 °C for 24 h. PVDF (average $M_w \sim$ 534 000 by GPC) was purchased from Sigma-Aldrich. Dimethyl sulfoxide (DMSO), *N*,*N*-dimethylformamide (DMF), and *N*,*N*-dimethylacetamide (DMAc) were purchased from Sinopharm Chemical Reagent Co., Ltd. (China).

Experimental Procedure. The SAIPE method reported previously was used to produce the PVDF/SWCNTs composites.[25−27] In a typical experiment, 0.5 mg of PVDF was dissolved in 4 g of DMSO at 150 °C. A 0.3 mg sample of SWCNTs was dispersed in 1 g of DMSO, and the mixture was ultrasonicated for 1 h before being added to the corresponding PVDF solution. The mixture was then quickly transferred into the SC CO_2 apparatus to reach the determined conditions of temperature and pressure. The time was controlled to 3 h for all samples. Control samples with different solvents for PVDF and SWCNTs, including DMF and DMAc, were prepared in a similar manner.

Characterization Methods. Transmission electron microscopy (TEM, FEI Tecnai G2 20) experiments were conducted with an accelerating voltage of 120 kV. IR spectra were collected on a TENSOR 27 FTIR spectrometer (Bruker) in the absorption mode with 32 scans at a resolution of 2 cm^{-1} intervals. Raman spectra were acquired using the sample in the solid state and were obtained at 514.5 nm laser excitation on a Renishaw Microscope System RM2000 at room temperature. Spectra were collected at various locations on each sample studied to determine reproducibility.

Results and Discussion

Dispersion of SWCNTs Modified with PVDF Using Different Solvents. In our previous study, we have successfully achieved the periodic patterning of PE on CNTs with the help of the supercritical CO_2 antisolvent effect. Considering PE as a type of polymer, it belongs to the concept of "soft matter" and they are characterized by a strong response to weak external fields and solution variables, and this response can induce structure change. The obtained PE/CNTs nanohybrid structure can be varied along with the variation of a series of experimental conditions or peripheral effects such as different solvents, PE concentration, CNTs concentration, and SC CO_2 pressure. Especially, it is evident that, compared to *p*-xylene used as the solvent, the decorated CNTs have more excellent dispersion, and the size and periodicity of the kebab structures are much larger in dichlorobenzene (DCB).[26] In the SAIPE procedure, the variation of solvents is a typical peripheral factor, which affects the antisolvent power and results in different modification effects. Therefore, in this study, we choose three organic solvents such as DMSO, DMF, and DMAc and study their effects on SC CO_2-induced PVDF epitaxy on SWCNTs.

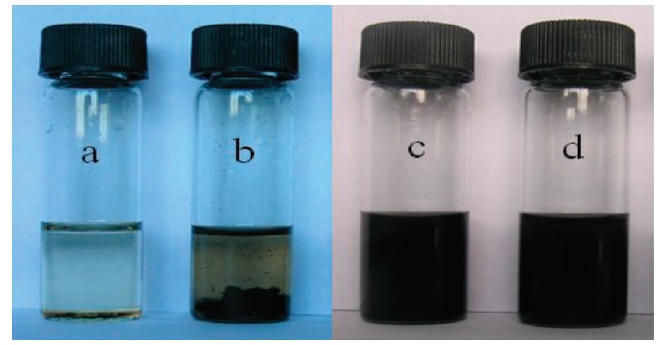

Figure 1. Photographs of four different samples: (a) SWCNTs/DMSO mixture after sonification; SWCNTs decorated with PVDF in DMSO (b), DMF (c), and DMAc (d) produced in SC CO_2 at 15 MPa/150 °C for 3 h.

TABLE 1: Solubility Parameters of PVDF and Three Solvents

	PVDF	DMSO	DMF	DMAc
solubility parameter/$(J/cm^3)^{1/2}$	23.2	27.4	24.8	22.7

The photographs of four different samples are shown in Figure 1. Sample a was prepared through ultrasonic vibration of SWCNTs in DMSO at 45 °C for 2 h. Samples b, c, and d were obtained by modifying SWCNTs with PVDF in DMSO, DMF, and DMAc, respectively, under the same SC CO_2 conditions (150 °C, 15 MPa, 3 h). All the samples were kept for more than 2 months before photographing. It can be seen in Figure 1a that a black precipitate of pure SWCNTs collects at the bottom of the vial due to their intrinsic poor solubility. The suspension of sample b appears to be stable without precipitation happening. However, apparently in Figure 1c,d, SWCNTs decorated with PVDF in DMF and DMAc have more excellent dispersion than that in DMSO. The solubility parameters of PVDF and the three organic solvents are provided in Table 1.[37,38] From Table 1, it can be found that the value of PVDF is 23.2 $(J/cm^3)^{1/2}$, which is closer to those of DMF (24.8) and DMAc (22.7) than that of DMSO (27.4). Considering CO_2 will be added into the solution as antisolvent, it is very necessary to study the miscibility of CO_2 in different solvents. The extent of miscibility is reflected in the volume expansion of the liquid phase after injection of condensed CO_2. And the volume expansion of the liquid phase $\Delta V/V_0$ at a certain pressure P and temperature T is defined by

$$\Delta V/V_0 = [V(P,T) - V(P^0,T)]/V(P^0,T) \quad (1)$$

The experimental results are shown in Figure 2. It can be observed that at 11 MPa or higher pressure, the miscibility of

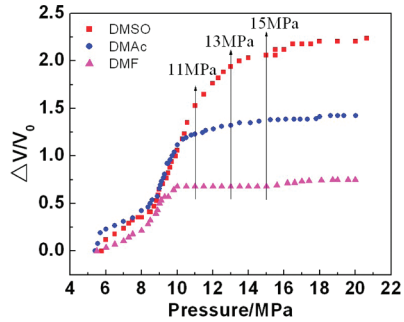

Figure 2. Volume expansion of three solutions of PVDF/DMSO, PVDF/DMF, and PVDF/DMAc in CO_2 as a function of pressure.

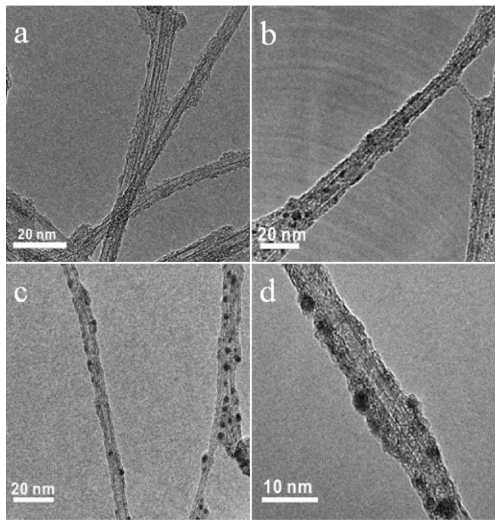

Figure 3. TEM images of PVDF decorated SWCNTs using DMSO as solvent, produced in the same PVDF concentration (0.01 wt %) and SWCNTs concentration (0.006 wt %) at 150 °C for 3 h, but at different SC CO_2 pressures: (a) 11 MPa; (b) 13 MPa; (c) and (d) 15 MPa.

CO_2 in DMSO is apparently higher than that in DMF and DMAc. That is, for the same PVDF concentration solution, CO_2 will exert more antisovent effect for PVDF/DMSO solution than that for PVDF/DMF and PVDF/DMAc solutions. It can be imagined when CO_2 was added, more PVDF will precipitate from DMSO solution compared to that from DMF and DMAc solutions. And the precipitated amount of PVDF will increase greatly with the increase of CO_2 pressure for the PVDF/DMSO solution system. Thus in the following study, we will investigate the decorated effect of PVDF on CNTs in the three organic solution systems and also study the effect of CO_2 pressure on PVDF modified CNTs for every solution system.

Modification of SWCNTs with PVDF Using DMSO as Solvent. Figure 3 shows the TEM micrographs of SWCNTs decorated with PVDF in DMSO at different SC CO_2 pressures. From Figure 3, it can be seen clearly that SWCNTs are wrapped by PVDF molecules. When the experimental pressure was as low as 11 MPa, a few of PVDF deposited on SWCNTs and the naked CNTs can be seen. With an increase of SC CO_2 pressure, the decorating degree of PVDF on the surface of SWCNTs increases significantly. When the experimental pressure reaches 15 MPa, some black dots are formed, the average diameters of which are in the range of 2−5 nm, and we call these dots as nanocrystals. As indicated in our previous study, the mechanism is attributed to a variation of antisolvent power with the increase of SC CO_2 pressure.[39] Namely, with an increasing of SC CO_2 pressure, the amount and speed of CO_2 dissolved in DMSO increase and the solvent power of DMSO decreases. Therefore,

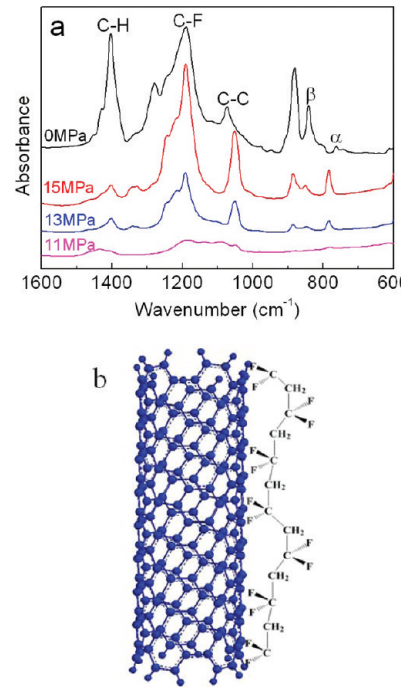

Figure 4. FTIR spectra of PVDF/SWCNTs/DMSO at different SC CO_2 pressures (a) and a schematic showing the interaction between PVDF and SWCNTs (b).

more PVDF can be deposited and the polymer chains would likely undergo transition from a loose coil to a dense globule so as to minimize polymer−solvent interactions in the poorer solvent. And this phenomenon is in accordance with the experimental results of miscibility shown in Figure 2.

It is known that CNTs are electron-rich molecules and any electron-deficient molecules can interact with them and form donor−acceptor complexes. And the $\pi-\pi$ interactions of CNTs with electron-rich molecules have been used for the noncovalent functionalization.[18,19,40−42] Furthermore, Baskaran et al. confirmed the presence of a weak noncovalent and nonspecific CH-π interaction between organic molecules (both small molecule and macromolecules) and CNTs, although the mechanism of intermolecular interaction and the physicochemical state of adsorbed molecules still needs further study.[43] To probe the molecular interaction between PVDF and CNTs, the composite mixtures were subjected to FT-IR analysis and the results are presented in Figure 4. For the sample prepared only by blending PVDF and SWCNTs in DMSO without treatment in SC CO_2 (0 MPa), the characteristic frequencies of PVDF can be clearly observed. Concretely, the peak at 1402 cm^{-1} represents the distortion vibration band of C−H, the peak at 1189 cm^{-1} is due to the stretching vibration band of C−F, and the peak at 1072 cm^{-1} is owing to the stretching vibration band of C−C. For the PVDF/SWCNTs samples prepared under different SC CO_2 conditions, when the pressure is as low as 11 MPa, the absorption intensity is very weak because only a few of PVDF decorating on SWCNTs and the characteristic frequencies of PVDF are hard to identify. With the increase of pressure, the absorption bands ascribed to PVDF are visible, confirming that more PVDF molecules are decorated on the surface of CNTs under the higher SC CO_2 pressure. In addition, it can be observed that the relative intensities of the peaks change obviously and the peak positions show displacement compared with the spectrum of PVDF/SWCNT/DMSO mixtures without treatment in SC CO_2 (0 MPa). For instance, at 15 MPa, the intensity of the C−F stretching vibration band is increased and

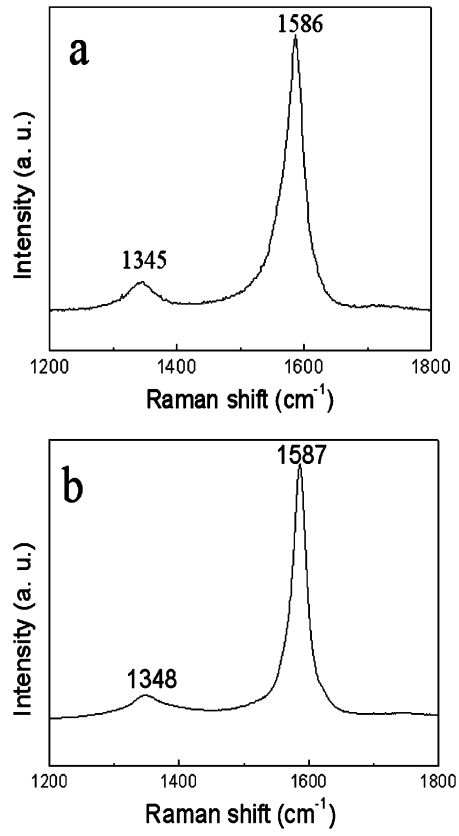

Figure 5. Raman spectra of the pristine SWCNT (a) and PVDF-decorated SWCNTs using DMSO as solvent, formed in PVDF concentration (0.01 wt %) and SWCNTs concentration (0.006 wt %), and at SC CO_2 conditions of 15 MPa/150 °C for 3 h (b), ($\lambda_{excitation}$ = 514.5 nm).

shifts 2 cm^{-1} to low wavenumber, and the C−C stretching vibration band is also strengthened and shifts about 20 cm^{-1} to low wavenumber. It implies that there may exist interaction between SWCNTs and PVDF chains.[44] In addition, the intensity of the C−H distortion vibration band at 1402 cm^{-1} is weakened significantly. It suggests that it is due to the nonspecific molecular interactions between the C−H groups of PVDF and CNTs, as reported in the literature.[43] A schematic showing the interaction between PVDF and SWCNTs is illustrated in Figure 4b.

The interfacial interactions between polymer and carbon materials, such as CNTs, have also been probed using Raman spectroscopy.[44−49] Raman spectra of pristine SWCNT and the corresponding PVDF-decorated SWCNTs at SC CO_2 conditions, recorded on a confocal Raman spectrometer using the laser excitation at 514.5 nm, are shown in Figure 5. The pristine SWCNTs has two characteristic peaks at 1345 and 1586 cm^{-1}, corresponding to the D-band (C−C, the disordered graphite structure) and G-band (C═C, sp^2-hybridized carbon), respectively.[45] The frequencies of the D-band and G-band of PVDF-decorated SWCNTs are slight shifted upward to 1348 and 1587 cm^{-1}, respectively. In addition, the I_D/I_G ratio was defined as the intensity ratio of the D-band to G-band of CNTs and directly indicated the structure changes of CNTs.[46] As listed in Table 2, the I_D/I_G ratio of pristine SWCNT was 0.095, while the I_D/I_G of the PVDF-decorated SWCNTs increased to 0.15. The higher I_D/I_G ratio and the upshift of D- and G-bands are in accord with the results reported by Huang et al. and Yang et al.[44,46] Huang et al. demonstrated that this phenomenon was attributed to a strong donor−acceptor interaction between the CNTs and

TABLE 2: Raman I_D/I_G Intensity Ratios and D- and G-Bands Shifts of Pristine SWCNTs and PVDF-Decorated SWCNTs Using DMSO as Solvent with SC CO_2 at 15 MPa

	SWCNT	PVDF/SWCNT
I_D/I_G	0.095	0.15
D-band (cm^{-1})	1345	1348
G-band (cm^{-1})	1586	1587

fuorine at the interfaces. Therefore, the FTIR and Raman spectra provide evidence that there exists a charge-transfer type of interaction between CNTs and the electron-withdrawing fluorine atoms on the PVDF chains.

Moreover, PVDF is known to be a semicrystalline polymer with five different polymorphs, α-, β-, γ-, δ-, and ε-forms.[31] The formation of these PVDF polymorphs strongly depends on the crystallization conditions and processing of the polymer. As can be seen from Figure 4a, for the sample without treatment in SC CO_2 (0 MPa), the typical absorption peaks attributed to the β-form at 765 cm^{-1} and the α-form at 840 cm^{-1} are both observed. And apparently the β-form is the predominant phase. However, for the sample treated with SC CO_2 (especially at 15 MPa), the absorption band of the α-phase is enhanced whereas the peak ascribed to the β-phase is weakened relatively; i.e., the α-phase became predominant due to the effect of SC CO_2. So it can be concluded that for the antisolvent effect of SC CO_2, it can help to precipitate the polymorphs from the solvent selectively. And, to some degree, the effect of SC CO_2 is similar to the action of the elongation/shear flow field, which can lead to the crystal phase transformation of the polymer reported in other research.[34] For PVDF, it is a semicrystalline polymer with two main crystal phases, the nonpolar α-phase and the polar β-phase. Because of the weak polarity of CO_2, it is inclined to help the nonpolar α-phase precipitate out and settle on CNTs. The α-phase is the alternating trans- and gauche-bond conformation with the helical structure. In our TEM characterization, we indeed can find the helical structure of PVDF wrapping on SWCNTs, which is shown in Figure 6.

Modification of SWCNTs with PVDF Using DMF as Solvent. Figure 7 displays the TEM micrographs of SWCNTs decorated with PVDF using DMF as the solvent at different SC CO_2 pressures. Apparently, it can be seen that PVDF molecular chains have been wrapping around CNTs. Compared

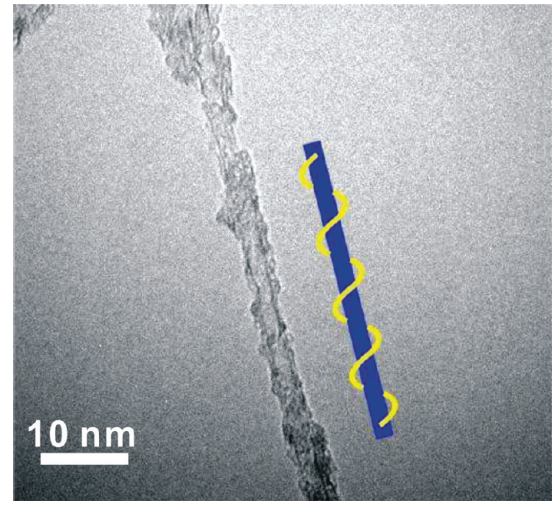

Figure 6. TEM image of PVDF-decorated SWCNTs using DMSO as solvent, formed with PVDF concentration of 0.01 wt % and SWCNTs concentration of 0.006 wt %, and at SC CO_2 conditions of 15 MPa/150 °C for 3 h.

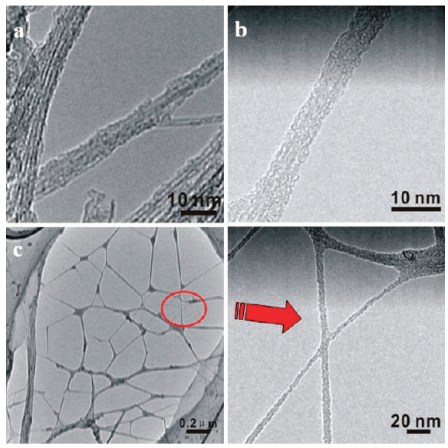

Figure 7. TEM images of PVDF-decorated SWCNTs using DMF as solvent, produced in the same PVDF concentration (0.01 wt %) and SWCNTs concentration (0.006 wt %) at 150 °C for 3 h, but at different SC CO_2 pressures: (a) 11 MPa; (b) 13 MPa; (c) 15 MPa.

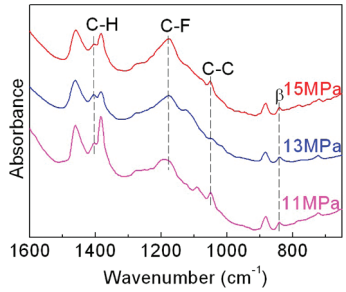

Figure 8. FTIR spectra of PVDF-decorated SWCNTs using DMF as solvent at different SC CO_2 pressures.

to the experimental results obtained using DMSO as solvent, there is no generation of nanocrystals in DMF. From Figure 2, it can be found that the miscibility of CO_2 in DMF is much weaker compared to that in DMSO. And there is no volume increase for the liquid phase of DMF with the increase of CO_2 pressure in the range of 11−15 MPa; i.e., the increase of CO_2 pressure cannot help to improve the solubility of CO_2 in DMF. However, in Figure 7c, we observe a novel phenomenon that when the SC CO_2 pressure reaches 15 MPa, the modified CNTs seem to be stretched by some sort of force and cross each other to form a typical network structure, which is similar to a spider web. This special morphology should be favorable to obtain high perfermance nanotube−PVDF composites when the modified CNTs act as a reinforcing fiber. It is suggested that the formation of the cobweb-like structure is attributed to two factors: one is the similar solubility parameters of PVDF (23.2 $(J/cm^3)^{1/2}$) and DMF (24.8 $(J/cm^3)^{1/2}$), and the other is the weak solubility of CO_2 in DMF when CO_2 is used as an antisolvent to help PVDF precipitate from DMF.

The FT-IR spectra of PVDF/SWCNTs/DMF mixtures treated at different conditions are shown in Figure 8. The characteristic absorption peaks of PVDF have been marked in Figure 8, and these peak positions also show displacement compared with those of the sample without treatment in SC CO_2. This result is similar to those using DMSO as the solvent and implies that there are multiple interactions between PVDF and CNTs even in DMF. However, it can be seen that the infrared spectra of PVDF decorated SWCNTs in DMF have no apparent changes with the variation of SC CO_2 pressure. In addition, for all samples prepared after SC CO_2 treatment, we can clearly observe the typical absorption peak ascribed to β-phase at 840 cm^{-1}, while the peak assigned to the α-phase is weak; i.e., there

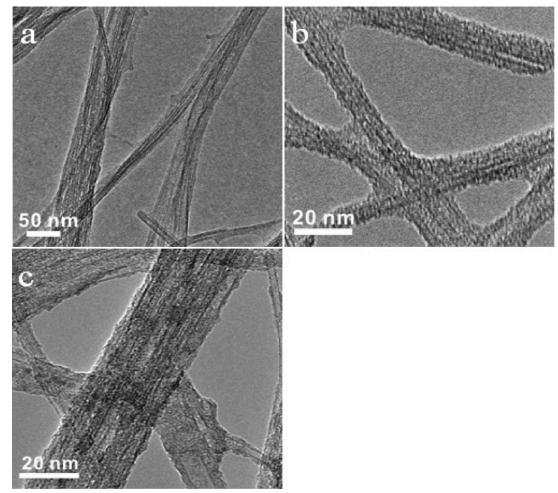

Figure 9. TEM images of PVDF-decorated SWCNTs using DMAc as solvent, produced in the same PVDF concentration (0.01 wt %) and SWCNTs concentration (0.006 wt %) at 150 °C for 3 h, but at different SC CO_2 pressures: (a) 11 MPa; (b) 13 MPa; (c) 15 MPa.

is no transformation between the β-form and α-form. It is totally different from the result discussed above when DMSO is used as solvent. It suggests that the effect of SC CO_2 on crystal transformation is related to the choice of solvent. In fact, due to the good dissolving power of DMF to PVDF, PVDF chains can fully extend in DMF and thus be favorable to form flat-serrated crystals; i.e., molecular chains exist in the form of β-phase along the stem of SWCNTs. So this is evidence that choosing the proper solvent can help to obtain the desired microstructures, which is closely interrelated to the properties of materials.

Modification of SWCNTs with PVDF Using DMAc as Solvent. From the photographs in Figure 1, it can be seen that PVDF modified CNTs in DMF and DMAc both have the excellent dispersion and exist in a homogeneous state for a long time. This is due to the close solubility parameter of PVDF with DMF and DMAc. And it can be observed from Figure 2 that the compatibility of CO_2 in DMAc lies between the DMSO and DMF. Figure 9 presents the TEM micrographs of SWCNTs decorated with PVDF at different SC CO_2 pressures when DMAc was used as the solvent. Because of the excellent miscibility of the PVDF/DMAc system, when the pressure of SC CO_2 is low, the antisolvent effect of SC CO_2 is weak and little PVDF precipitates from solution. With the increase of SC CO_2 pressure from 11 to 15 MPa, the coating of PVDF on SWCNTs became thicker. However, being similar to the result using DMF as solvent, there is no generation of nanocrystals even when the SC CO_2 pressure reaches 15 MPa. In comparison with the FT-IR spectra of the PVDF/SWCNTs/DMAc system, we also focus on the transformation of the α-form and β-form. Upon close examination of the infrared spectra in Figure 10, the peak attributed to the β-form at 840 cm^{-1} can be observed while the peak ascribed to the α-form is hard to detect. This indicates that using DMAc as the solvent for PVDF/SWCNTs cannot help to improve the content of the α-form during the process of SC CO_2.

By comparing the experimental results using DMSO, DMF, and DMAc as solvents for PVDF, we can conclude that the choice of solvent is important to obtain the specific microstructure and the desired property of PVDF modified CNTs. The desired modification effect of PVDF on CNTs can be determined by choosing the solvent with proper dissolving power for the polymer, and with suitable compatibility with CO_2 as well.

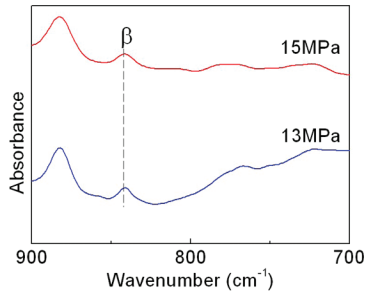

Figure 10. FTIR spectra of PVDF-decorated SWCNTs using DMAc as solvent at different SC CO_2 pressures.

Conclusions

In this study, wrapping SWCNTs with a kind of piezoelectric polymer, PVDF, was obtained by the SC CO_2 antisolvent technique, and the impact of various solvents on the decoration effect was studied. Our experimental results are illustrated as follows: When DMSO was used as the solvent, the decorating degree of PVDF on the surface of SWCNTs increased significantly with the increase of the SC CO_2 pressure, and the nanohybrid structure with nanocrystals wrapping on SWCNTs was formed at 15 MPa. The FTIR and Raman spectra provided the evidence that there exists a charge-transfer type of interaction between CNTs and the electron-withdrawing fluorine atoms on the PVDF chains. In addition, FTIR results showed that there exists a transformation from the β-phase to the α-phase of PVDF in DMSO with the assistance of SC CO_2, and accordingly, the helical structure of PVDF wrapping on SWCNTs was observed. And this structure was a reflection of the alternating trans- and gauche-bond conformation of the α-form. When DMF or DMAc was used as the solvent, SWCNTs have more excellent dispersion than that in DMSO. When DMF was used as the solvent, a typical spider net structure was observed, which should be helpful to obtain the high perfermance nanotube−PVDF composite. This supplies a clue for us that the variation of solvent has a decisive effect on the micro- morphology and crystallization of polymer decorating on CNTs, and consequently, the obtained PVDF/CNTs can be applied in various areas of manufacture.

Acknowledgment. We are grateful for the National Natural Science Foundation of China (No. 20974102) and the financial support from the Program for New Century Excellent Talents in University (NCET).

References and Notes

(1) Iijima, S. *Nature* **1991**, *354*, 56.
(2) Gao, C. *Macromol. Rapid Commun.* **2006**, *27*, 841.
(3) Moniruzzaman, M.; Winey, K. I. *Macromolecules* **2006**, *39*, 5194.
(4) Kim, J. A.; Seong, D. G.; Kang, T. J.; Youn, J. R. *Carbon* **2006**, *44*, 1898.
(5) Kuila, B. K.; Malik, S.; Batabyal, S. K.; Nandi, A. K. *Macromolecules* **2007**, *40*, 278.
(6) Uragami, T.; Katayama, T.; Miyata, T.; Tamura, H.; Shiraiwa, T.; Higuchi, A. *Biomacromolecules* **2004**, *5*, 1567.
(7) Liu, Y. Q.; Gao, L. *Carbon* **2005**, *43*, 47.
(8) Kyotani, T.; Nakazaki, S.; Xu, W.; Tomita, A. *Carbon* **2001**, *39*, 782.
(9) Mawhinney, D. B.; Naumenko, V.; Kuznetsova, A.; Yates, J. T.; Liu, J.; Smalley, R. E. *Chem. Phys. Lett.* **2000**, *324*, 213.
(10) Sham, M. L.; Kim, J. K. *Carbon* **2006**, *44*, 768.
(11) Fu, D. L.; Xu, Y. P.; Li, L. J.; Chen, Y.; Mhaisalkar, S. G.; Boey, F. Y. C.; Lin, T. W.; Moochhala, S. *Carbon* **2007**, *45*, 1911.
(12) Hirsch, A. *Angew. Chem., Int. Ed.* **2002**, *41*, 1853.
(13) Liu, Y.; Tang, J.; Chen, X.; Xin, J. *Carbon* **2005**, *43*, 3178.
(14) O'Connell, M. J.; Boul, P.; Ericson, L. M.; Huffman, C.; Wang, Y.; Haroz, E.; Kuper, C.; Tour, J.; Ausman, K. D.; Smalley, R. E. *Chem. Phys. Lett.* **2001**, *342*, 265.
(15) Wang, J.; Musameh, M.; Lin, Y. *J. Am. Chem. Soc.* **2003**, *125*, 2408.
(16) Star, A.; Stoddart, J. F.; Steuerman, D.; Diehl, M.; Boukai, A.; Wong, E. W.; Yang, X.; Chung, S. W.; Choi, H.; Heath, J. R. *Angew. Chem., Int. Ed.* **2001**, *40*, 1721.
(17) Dieckmann, G. R.; Dalton, A. B.; Johnson, P. A.; Razal, J.; Chen, J.; Giordano, G. M.; Munoz, E.; Musselman, I. H.; Baughman, R. H.; Draper, R. K. *J. Am. Chem. Soc.* **2003**, *125*, 1770.
(18) Chen, R.; Zhang, Y.; Wang, D.; Dai, H. *J. Am. Chem. Soc.* **2001**, *123*, 3838.
(19) Zhang, J.; Lee, J. K.; Wu, Y.; Murray, R. W. *Nano Lett.* **2003**, *3*, 403.
(20) Eckert, C. A.; Knutson, B. L.; Debendetti, P. G. *Nature* **1996**, *383*, 313.
(21) Britz, D. A.; Khlobystov, A. N.; Wang, J.; O'Neil, A. S.; Poliakoff, M.; Ardavan, A.; Briggs, G. A. D. *Chem. Commun.* **2004**, 176.
(22) Ye, X. R.; Lin, Y.; Wang, C.; Wai, C. M. *Adv. Mater.* **2003**, *15*, 316.
(23) Tomasko, D. L.; Li, H.; Liu, D.; Han, X.; Wingert, M. J.; James Lee, L.; Koelling, K. W. *Ind. Eng. Chem. Res.* **2003**, *42*, 6431.
(24) Dai, X.; Liu, Z.; Han, B.; Sun, Z.; Wang, Y.; Xu, J.; Guo, X.; Zhao, N.; Chen, J. *Chem. Commun.* **2004**, 2190.
(25) Yue, J.; Xu, Q.; Zhang, Z.; Chen, Z. *Macromolecules* **2007**, *40*, 8821.
(26) Zhang, Z.; Xu, Q.; Chen, Z.; Yue, J. *Macromolecules* **2008**, *41*, 2868.
(27) Zhang, F.; Zhang, H.; Zhang, Z.; Chen, Z.; Xu, Q. *Macromolecules* **2008**, *41*, 4519.
(28) Yang, Y.; Wu, G.; Ramalingam, S.; Hsu, S. L.; Kleiner, L.; Tang, F. *Macromolecules* **2007**, *40*, 9658.
(29) Priya, L.; Jog, J. P. *J. Polym. Sci., Part B: Polym. Phys.* **2002**, *40*, 1682.
(30) Lang, S. B.; Muensit, S. *Appl. Phys. A: Solids Surf.* **2006**, *85*, 125.
(31) Lovinger, A. J. *Science* **1983**, *220*, 1115.
(32) Maier, G. A.; Wallner, G.; Lang, R. W; Fratzl, P. *Macromolecules* **2005**, *38*, 6099.
(33) Kim, D.; Sun, Y.; Yun, S.; Lee, S.; Kim, B. *J. Biomechanics* **2005**, *38*, 1359.
(34) Sajkiewicz, P.; Wasiak, A.; Goclowski, Z. *Eur. Polym. J.* **1999**, *35*, 423.
(35) Imran-ul-haq, M.; Tiersch, B.; Beuermann, S. *Macromolecules* **2008**, *41*, 7453.
(36) Shieh, Y. T.; Hsiao, T. T.; Chang, S K. *Polymer* **2006**, *47*, 5929.
(37) Gao, C.; Xi, D.; Yang, X; Meng, Y. *Membr. Sci. Technol.* **2006**, *26*, 21.
(38) He, M.; Chen, W.; Dong, X. *Polym. Phys.* **2009**, 117.
(39) Zhang, F.; Xu, Q.; Zhang, H.; Zhang, Z. W. *J. Phys. Chem. C* **2009**, *113*, 18531.
(40) Kondratyuk, P.; Yates, J. T., Jr. *Chem. Phys. Lett.* **2004**, *383*, 314.
(41) Li, H.; Zhou, B.; Lin, Y.; Gu, L.; Wang, W.; Fernando, S.; Kumar, S.; Allard, L. F.; Sun, Y. P. *J. Am. Chem. Soc.* **2004**, *126*, 1014.
(42) Zhao, J.; Lu, J.; Han, J.; Yang, C. *Appl. Phys. Lett.* **2003**, *82*, 3746.
(43) Baskaran, D.; Mays, J. W.; Bratcher, M. S. *Chem. Mater.* **2005**, *17*, 3389.
(44) Huang, S.; Yee, W. A.; Tjiu, W. C.; Liu, Y.; Kotaki, M.; Boey, Y. C. F.; Ma, J.; Liu, T.; Lu, X. *Langmuir* **2008**, *24*, 13621.
(45) Price, B. K.; Hudson, J. L.; Tour, J. M. *J. Am. Chem. Soc.* **2005**, *127*, 14867.
(46) Yang, Q.; Shuai, L.; Pan, X. *Biomacromolecules* **2008**, *9*, 3422.
(47) Owens, F. J.; Jayakody, J. R. P.; Greenbaum, S. G. *Compos. Sci. Technol.* **2006**, *66*, 1280.
(48) Zhang, L.; Kiny, V. U.; Peng, H.; Zhu, J.; Lobo, R. F. M.; Margrave, J. L.; Khabashesku, V. N. *Chem. Mater.* **2004**, *16*, 2055.
(49) Li, Y.; Lee, E. J.; Cai, W. P.; Kim, K. Y.; Cho, S. O. *ACS Nano* **2008**, *2*, 1108.

JP911621Y